

July 2004

Flavour Structure and Proton Decay in 6D Orbifold GUTs

W. Buchmüller¹, L. Covi²,
D. Emmanuel-Costa³, S. Wiesenfeldt¹

¹ Deutsches Elektronen-Synchrotron DESY, Hamburg, Germany

² Theory Division, CERN Department of Physics, Geneva, Switzerland

³ CFTP, Departamento de Física, Instituto Superior Técnico, Lisbon, Portugal

Abstract

We study proton decay in a supersymmetric $\text{SO}(10)$ gauge theory in six dimensions compactified on an orbifold. The dimension-5 proton decay operators are forbidden by R-symmetry, whereas the dimension-6 operators are enhanced due to the presence of KK towers. Three sequential quark-lepton families are localised at the three orbifold fixed points, where $\text{SO}(10)$ is broken to its three GUT subgroups. The physical quarks and leptons are mixtures of these brane states and additional bulk zero modes. This leads to a characteristic pattern of branching ratios in proton decay, in particular the suppression of the $p \rightarrow \mu^+ K^0$ mode.

1 Introduction

The most striking consequence of Grand Unified Theories is proton decay [1–6]. It has been predicted and sought for more than 30 years, and its absence constitutes a very strong constraint on any realistic GUT model.

Recently, the discussion of proton decay has been revitalised on two different fronts. On the experimental side, the bounds coming from the SuperKamiokande experiment have reached $\tau(p \rightarrow e^+\pi^0) \geq 5.3 \times 10^{33}$ yrs [7] and $\tau(p \rightarrow K^+\bar{\nu}) \geq 1.9 \times 10^{33}$ yrs [8]. On the theoretical side, these bounds have motivated new detailed studies of proton decay via dimension-5 operators in supersymmetric SU(5) models [9–13]. These analyses showed that the present bounds disfavour this class of models, although the theoretical predictions strongly depend on the flavour structure assumed [12, 13].

Dimension-6 operators are less dangerous and have not drawn so much attention in the literature. It is, however, well known that such operators depend on the flavour structure as well [14–16], and it has been realised that the observed leptonic mixing can have a strong effect on the proton decay branching ratios [17]. Recently, dimension-6 operators have been studied in flipped SU(5) [18] and SO(10) [17, 19] GUTs.

The interest in dimension-6 operators has been renewed by GUT models in higher dimensions, with symmetry breaking via orbifolds. Here dimension-5 proton decay is naturally absent [20, 21]. In such models though, the dimension-6 operators are enhanced compared to the usual 4D case, due to the lower mass scale for the heavy particles mediating the decay and the presence of Kaluza-Klein towers of such states. Furthermore, the proton decay branching ratios depend on the localization of quarks and leptons [22].

The goal of the present paper is to study proton decay via dimension-6 operators in a specific SO(10) orbifold GUT model in 6D, where the complete Standard Model flavour structure can be reproduced via mixing of brane states with bulk split multiplets [23]. This kind of model can naturally arise in compactifications of the heterotic string [24, 25]. Quark and lepton mass matrices are approximately of lopsided type, with some characteristic modifications compared to the 4D lopsided picture. The up quark of the first generation is located on a brane where the bulk gauge group SO(10) is broken to SU(5) \times U(1), and therefore SU(5) gauge boson exchange gives the main contribution to proton decay. For this model, we will calculate the total rate and the branching ratios of proton decay and compare the results with those in a 4D SU(5) models with U(1) family symmetry.

The paper is organised as follows: in Section 2, we discuss the flavour structure of the 6D orbifold GUT model and evaluate the mixing matrices needed to calculate proton decay widths. Section 3 deals with proton decay via dimension-6 operators in the

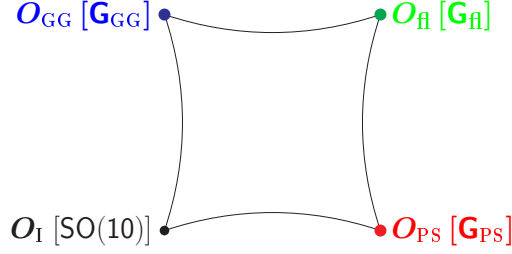


Figure 1: The three $\text{SO}(10)$ subgroups at the corresponding fixed points (branes) of the orbifold $T^2/Z_2 \times Z'_2 \times Z''_2$.

usual 4D case as well as the 6D model for which the sum over the Kaluza-Klein tower is performed. Finally, in Section 4 we discuss the effects of the flavour structure on the proton decay branching ratios in the different models. Conclusions are given in Section 5.

2 6D orbifold GUT model

We start from an $\text{SO}(10)$ gauge theory in 6D with $N = 1$ supersymmetry compactified on the orbifold $T^2/(Z_2^I \times Z_2^{\text{PS}} \times Z_2^{\text{GG}})$ [26,27]. The theory has four fixed points, O_I , O_{PS} , O_{GG} and O_{fl} , located at the four corners of a ‘pillow’ corresponding to the two compact dimensions (cf. Fig. 1). At O_I , only SUSY is broken, whereas at the other fixed points, O_{PS} , O_{GG} and O_{fl} , also $\text{SO}(10)$ is broken to its three GUT subgroups $\text{G}_{\text{PS}} = \text{SU}(4) \times \text{SU}(2) \times \text{SU}(2)$ [1], $\text{G}_{\text{GG}} = \text{SU}(5) \times \text{U}(1)_X$ [2] and flipped $\text{SU}(5)$ [5,6], $\text{G}_{\text{fl}} = \text{SU}(5)' \times \text{U}(1)'$, respectively. The intersection of all these GUT groups yields the standard model group with an additional $\text{U}(1)$ factor, $\text{G}_{\text{SM}'} = \text{SU}(3) \times \text{SU}(2) \times \text{U}(1)_Y \times \text{U}(1)_{Y'}$, as unbroken gauge symmetry below the compactification scale.

The field content of the theory is strongly constrained by imposing the cancellation of irreducible bulk and brane anomalies [28,29]. We study the model proposed in [23], containing three **16**-plets ψ_i , $i = 1, \dots, 3$, as brane fields, and six **10**-plets, H_1, \dots, H_6 , and four **16**-plets, $\Phi, \Phi^c, \phi, \phi^c$, as bulk hypermultiplets. Vacuum expectation values of Φ and Φ^c break the surviving $\text{U}(1)_{B-L}$. The electroweak gauge group is broken by expectation values of the anti-doublet and doublet contained in H_1 and H_2 .

We choose the parities of H_5 , H_6 and ϕ, ϕ^c such that their zero modes are

$$L = \begin{pmatrix} \nu_4 \\ e_4 \end{pmatrix}, \quad L^c = \begin{pmatrix} \nu_4^c \\ e_4^c \end{pmatrix}, \quad G_5^c = d_4^c, \quad G_6 = d_4. \quad (1)$$

These zero modes act as a (vectorial) fourth generation of down quarks and leptons and mix with the three generations of brane fields. We allocate the three sequential **16**-plets to the three branes where $\text{SO}(10)$ is broken to its three GUT subgroups, and place ψ_1 at

O_{GG} , ψ_2 at O_{fl} and ψ_3 at O_{ps} . The three ‘families’ are then separated by distances large compared to the cutoff scale M_* . Hence, they can only have diagonal Yukawa couplings with the bulk Higgs fields. Direct mixings are exponentially suppressed. The brane fields, however, can mix with the bulk zero modes for which we expect no suppression. These mixings take place only among left-handed leptons and right-handed down-quarks. This leads to a characteristic pattern of mass matrices.

As described in [23], after $B-L$ breaking at the scale v_N and electroweak symmetry breaking via $v_1 = \langle H_1^c \rangle$, $v_2 = \langle H_2 \rangle$, the mass terms assume the characteristic form

$$W = d_\alpha m_{\alpha\beta}^d d_\beta^c + e_\alpha^c m_{\alpha\beta}^e e_\beta + n_\alpha^c m_{\alpha\beta}^D \nu_\beta + u_i m_i^u u_i^c + \frac{1}{2} n_i^c m_i^N n_i^c, \quad (2)$$

where the Greek indices, $\alpha = 1 \dots 4$, include also the bulk states with $n_4^c = \nu_4^c$, while Latin indices only run over brane fields, $i = 1 \dots 3$. Note that there is no Majorana mass for $n_4^c = \nu_4^c$ which originates from the 6D hypermultiplet. m^u and m^N are diagonal 3×3 matrices ($\tan \beta = v_2/v_1$),

$$\frac{1}{\tan \beta} m^u \sim \frac{v_1 M_*}{v_N^2} m^N \sim \begin{pmatrix} \mu_1 & 0 & 0 \\ 0 & \mu_2 & 0 \\ 0 & 0 & \mu_3 \end{pmatrix}, \quad (3)$$

whereas m^d , m^e and m^D are 4×4 matrices with the common structure,

$$\frac{1}{\tan \beta} m^D \sim m^d \sim m^e \sim \begin{pmatrix} \mu_1 & 0 & 0 & \widetilde{\mu}_1 \\ 0 & \mu_2 & 0 & \widetilde{\mu}_2 \\ 0 & 0 & \mu_3 & \widetilde{\mu}_3 \\ \widetilde{M}_1 & \widetilde{M}_2 & \widetilde{M}_3 & \widetilde{M}_4 \end{pmatrix} \equiv m. \quad (4)$$

Here $\mu_i, \widetilde{\mu}_i = \mathcal{O}(v_1)$ and $\widetilde{M}_i = \mathcal{O}(GUT)$. The diagonal and the off-diagonal elements of these matrices satisfy several relations due to the underlying GUT symmetries [23]. The hypothesis of a universal strength of Yukawa couplings at each fixpoint leads to the identification of the diagonal and off-diagonal elements of $m^u/\tan \beta$, m^d , m^e and $m^D/\tan \beta$ up to coefficients of order one. This implies an approximate top-bottom unification with large $\tan \beta$ and a parametrization of quark and lepton mass hierarchies in terms of the six parameters μ_1, μ_2, μ_3 and $\widetilde{\mu}_1, \widetilde{\mu}_2, \widetilde{\mu}_3$.

The crucial feature of the matrices m^d , m^e and m^D are the mixings between the six brane states and the two bulk states. The first three rows of the matrices are proportional to the electroweak scale. The corresponding Yukawa couplings have to be hierarchical in order to obtain a realistic spectrum of quark and lepton masses. In a complete theory, this hierarchy may be due to the different location of the fixpoints on the orbifold. The fourth row, \widetilde{M}_α , is of order the unification scale and, as we assume, non-hierarchical.

The mass matrix m (cf. Eq. (4)) can be diagonalised by the unitary transformation

$$m = U_4 U_3 D V_3^\dagger V_4^\dagger, \quad (5)$$

where the matrices U_4, V_4 single out the heavy mass eigenstate, that can then be integrated out, while the matrices U_3, V_3 act only on the SM flavour indices and perform the final diagonalisation in the remaining 3×3 subspace. U_4 and V_4 are given by (neglecting phases)

$$U_4 = \begin{pmatrix} 1 & 0 & 0 & \frac{\mu_1 \widetilde{M}_1 + \tilde{\mu}_1 \widetilde{M}_4}{\widetilde{M}^2} \\ 0 & 1 & 0 & \frac{\mu_2 \widetilde{M}_2 + \tilde{\mu}_2 \widetilde{M}_4}{\widetilde{M}^2} \\ 0 & 0 & 1 & \frac{\mu_3 \widetilde{M}_3 + \tilde{\mu}_3 \widetilde{M}_4}{\widetilde{M}^2} \\ -\frac{\mu_1 \widetilde{M}_1 + \tilde{\mu}_1 \widetilde{M}_4}{\widetilde{M}^2} & -\frac{\mu_2 \widetilde{M}_2 + \tilde{\mu}_2 \widetilde{M}_4}{\widetilde{M}^2} & -\frac{\mu_3 \widetilde{M}_3 + \tilde{\mu}_3 \widetilde{M}_4}{\widetilde{M}^2} & 1 \end{pmatrix} + \mathcal{O}\left(\frac{v^2}{\widetilde{M}^2}\right), \quad (6)$$

$$V_4 = \begin{pmatrix} \frac{\widetilde{M}_4}{\widetilde{M}_{14}} & 0 & -\frac{\widetilde{M}_1 \widetilde{M}_{23}}{\widetilde{M} \widetilde{M}_{14}} & \frac{\widetilde{M}_1}{\widetilde{M}} \\ 0 & \frac{\widetilde{M}_3}{\widetilde{M}_{23}} & \frac{\widetilde{M}_2 \widetilde{M}_{14}}{\widetilde{M} \widetilde{M}_{23}} & \frac{\widetilde{M}_2}{\widetilde{M}} \\ 0 & -\frac{\widetilde{M}_2}{\widetilde{M}_{23}} & \frac{\widetilde{M}_3 \widetilde{M}_{14}}{\widetilde{M} \widetilde{M}_{23}} & \frac{\widetilde{M}_3}{\widetilde{M}} \\ -\frac{\widetilde{M}_1}{\widetilde{M}_{14}} & 0 & -\frac{\widetilde{M}_4 \widetilde{M}_{23}}{\widetilde{M} \widetilde{M}_{14}} & \frac{\widetilde{M}_4}{\widetilde{M}} \end{pmatrix}, \quad (7)$$

where $\widetilde{M} = \sqrt{\sum_\alpha \widetilde{M}_\alpha^2}$ and $\widetilde{M}_{\alpha\beta} = \sqrt{\widetilde{M}_\alpha^2 + \widetilde{M}_\beta^2}$. In general, V_4 contains large mixings, while U_4 is approximately the unit matrix up to corrections $\mathcal{O}(v/\widetilde{M})$. U_3 and V_3 are the matrices that diagonalise

$$m' = U_4^\dagger m V_4 = \begin{pmatrix} \widehat{m} & 0 \\ 0 & \widetilde{M} \end{pmatrix} + \mathcal{O}\left(\frac{v^2}{\widetilde{M}}\right), \quad (8)$$

where

$$\widehat{m} = \begin{pmatrix} \mu_1(V_4)_{1j} + \tilde{\mu}_1(V_4)_{4j} \\ \mu_2(V_4)_{2j} + \tilde{\mu}_2(V_4)_{4j} \\ \mu_3(V_4)_{3j} + \tilde{\mu}_3(V_4)_{4j} \end{pmatrix}. \quad (9)$$

Clearly, they have only a non-trivial 3×3 part,

$$U_3 = \begin{pmatrix} V_{\text{CKM}}^\dagger & 0 \\ 0 & 1 \end{pmatrix}, \quad V_3 = \begin{pmatrix} \widehat{V} & 0 \\ 0 & 1 \end{pmatrix}. \quad (10)$$

Notice that the rows of \widehat{m} scale each like $\mu_i, \tilde{\mu}_i$. Hence, for hierarchical parameters $\mu_1, \tilde{\mu}_1 < \mu_2, \tilde{\mu}_2 < \mu_3, \tilde{\mu}_3$ we obtain a structure familiar from lopsided fermion mass models.

As discussed in [23], we can choose the parameters in such a way to give a consistent quark mass pattern and CKM matrix, in particular

$$\mu_1 : \mu_2 : \mu_3 \sim m_u : m_c : m_t , \quad (11)$$

and (cf. Eq. (17))

$$\bar{\mu}_3 \simeq m_b , \quad \tilde{\mu}_2 : \bar{\mu}_3 \sim m_s : m_b . \quad (12)$$

The CKM matrix in U_3 arises in a natural way as well. Setting the remaining parameter $\tilde{\mu}_1$ to give

$$V_{us} = \Theta_c \simeq \frac{\tilde{\mu}_1}{\tilde{\mu}_2} \simeq 0.2 , \quad (13)$$

the other matrix elements are determined by the quark masses [23],

$$V_{cb} \sim \frac{\tilde{\mu}_2}{\tilde{\mu}_3} \simeq \frac{m_s}{m_b} \simeq 2 \times 10^{-2} , \quad V_{ub} \sim \frac{\tilde{\mu}_1}{\tilde{\mu}_3} = \Theta_c \frac{m_s}{m_b} \simeq 4 \times 10^{-3} . \quad (14)$$

Within the accuracy of our approach this is consistent with the analysis from weak decays [30].

The matrix \hat{V} takes a relatively simple form in the case when $\mu_{1,2} = 0$ and the mass matrix in Eq. (9) has one zero eigenvalue. We then obtain

$$\hat{V} = \begin{pmatrix} -\frac{\tilde{M}_2 \tilde{M}_4}{\tilde{M}_{12} \tilde{M}_{14}} & \frac{\tilde{M}_1 (\tilde{\mu}_3 \tilde{M}_3 \tilde{M}_4 - \mu_3 (\tilde{M}_1^2 + \tilde{M}_2^2 + \tilde{M}_4^2))}{\tilde{\mu}_3 \tilde{M} \tilde{M}_{12} \tilde{M}_{14}} & -\frac{\tilde{\mu}_3 \tilde{M}_1}{\tilde{\mu}_3 \tilde{M}_{14}} \\ \frac{\tilde{M}_1 \tilde{M}_3}{\tilde{M}_{12} \tilde{M}_{23}} & \frac{\tilde{M}_2 (\tilde{\mu}_3 (\tilde{M}_1^2 + \tilde{M}_2^2 + \tilde{M}_3^2) - \mu_3 \tilde{M}_3 \tilde{M}_4)}{\tilde{\mu}_3 \tilde{M} \tilde{M}_{12} \tilde{M}_{23}} & -\frac{\mu_3 \tilde{M}_2}{\tilde{\mu}_3 \tilde{M}_{23}} \\ \frac{\tilde{M}_1 \tilde{M}_2 \tilde{M}}{\tilde{M}_{12} \tilde{M}_{14} \tilde{M}_{23}} & -\frac{\tilde{\mu}_3 \tilde{M}_1^2 \tilde{M}_3 + \mu_3 \tilde{M}_2^2 \tilde{M}_4}{\tilde{\mu}_3 \tilde{M}_{12} \tilde{M}_{14} \tilde{M}_{23}} & -\frac{\tilde{\mu}_3 \tilde{M}_4 \tilde{M}_{23}}{\tilde{\mu}_3 \tilde{M} \tilde{M}_{14}} + \frac{\mu_3 \tilde{M}_3 \tilde{M}_{14}}{\tilde{\mu}_3 \tilde{M} \tilde{M}_{23}} \end{pmatrix} , \quad (15)$$

up to a two-dimensional mixing matrix for the second and third generation, parameterized by a small angle Θ_R ,

$$\Theta_R \simeq \frac{\tilde{\mu}_1^2 + \tilde{\mu}_2^2}{\bar{\mu}_3^2} \ll 1 , \quad (16)$$

where we have defined

$$\bar{\mu}_3^2 = \tilde{\mu}_3^2 \left(1 - \frac{\tilde{M}_4^2}{\tilde{M}^2} \right) + \mu_3^2 \left(1 - \frac{\tilde{M}_3^2}{\tilde{M}^2} \right) - 2\mu_3 \tilde{\mu}_3 \frac{\tilde{M}_3 \tilde{M}_4}{\tilde{M}^2} . \quad (17)$$

The case of small $\mu_{1,2}$ limit is actually of physical relevance, since it gives for the down quark

$$\frac{m_d}{m_s} \sim \frac{\mu_2}{\tilde{\mu}_2} \frac{\tilde{\mu}_1}{\tilde{\mu}_2} \sim \Theta_c \frac{m_c m_b}{m_t m_s} \simeq 0.03 , \quad (18)$$

consistent with data [31]. Since $\mu_2/\tilde{\mu}_2 \sim m_c m_b/(m_t m_s) \sim 0.1$, the corrections to the matrix (15) are small.

The charged lepton mass matrix m^e has the same structure as the down-quark mass matrix, but there the large mixings are between the ‘left-handed’ states e_i . Experimental data require for the largest eigenvalue $m_\tau \simeq m_b$, whereas the second and the third eigenvalue have to satisfy the relations $m_\mu \simeq 3m_s$ and $m_e \simeq 0.2m_d$, respectively. This is consistent with our identification of m^d and m^e up to coefficients of order one unless the relevant parameters are fixed by GUT relations. The comparison between the expression (18) for m_d and the corresponding one for m_e suggests locating the second family on the flipped SU(5) brane. The successful relation for the light neutrino mass, $m_3 \sim m_t^2/M_3 \sim m_t^2 M_*/v_N^2 \sim 0.01$ eV, requires the third family to be located on the PS brane. With the first family on the GG brane, m_d and m_e are determined by the parameters μ_2^d and μ_2^e , which are not related by a flipped SU(5) mass relation.

3 Proton decay via dimension-6 operators

3.1 Effective SU(5) operators in 4D models

Dimension-6 proton decay in the SU(5) model is mediated by the exchange of the X and Y leptoquark gauge bosons [16]. Contrary to the dimension-5 operator, it does not involve any dressing through supersymmetric partners and therefore it is not sensitive to the supersymmetry breaking scale (except for the weak dependence of the GUT scale on the superparticle mass spectrum). The effective vertex is obtained by simply integrating out the heavy gauge bosons.

The couplings of the SU(5) representations $\mathbf{5}^*$ and $\mathbf{10}$ with the SU(5) gauge bosons are given by their kinetic terms,

$$\int_{\theta^2 \bar{\theta}^2} \sum_{\text{reps}} \bar{\Phi}_i e^{2V} \Phi_i, \quad (19)$$

which include

$$\mathcal{L} = i \frac{g_5}{\sqrt{2}} A_\mu^a \left[2 \text{tr} (\overline{\mathbf{10}}_i \gamma^\mu T^a \mathbf{10}_i) + \bar{\mathbf{5}}_k^* \gamma^\mu (T^a)^\top \mathbf{5}_k^* \right] + \text{h.c.}, \quad (20)$$

where g_5 is the SU(5) gauge coupling; the Latin indices count the generations, $i = 1 \dots 3$ those of $\mathbf{10}$, $k = 1 \dots 3$ those of $\mathbf{5}^*$.

We now express the SU(5) representations in terms of SM fields with $\mathcal{X} = (X, Y)$ being a $(\mathbf{3}^*, \mathbf{2}, 5/6)$ representation of $\text{SU}(3) \times \text{SU}(2) \times \text{U}(1)$. This yields the baryon and

lepton number violating terms

$$\mathcal{L} = -i \frac{g_5}{\sqrt{2}} \mathcal{X}_{\alpha\mu} [\epsilon_{\alpha\beta\gamma} \bar{Q}_{\beta,i} \gamma^\mu u_{\gamma,i}^c + \bar{e}_i^c \gamma^\mu Q_{\alpha,i} - \bar{d}_{\alpha,k}^c \gamma^\mu L_k] + \text{h.c.} , \quad (21)$$

where Greek indices denote the colour degrees of freedom and the SU(2) indices have been suppressed. Note that the first two terms come from the **10** representation, the last one from the **5**^{*}.

Integrating out the heavy gauge bosons with masses $M_{\mathcal{X}}$, we get the effective operators relevant for proton decay

$$\mathcal{L}_{\text{eff}} = -\frac{g_5^2}{2M_{\mathcal{X}}^2} \epsilon_{\alpha\beta\gamma} \bar{u}_{\alpha,i}^c \gamma^\mu Q_{\beta,i} [\bar{e}_j^c \gamma_\mu Q_{\gamma,j} - \bar{d}_{\gamma,k}^c \gamma_\mu L_k] + \text{h.c.} . \quad (22)$$

With Fierz reordering, one can write the operators as

$$\mathcal{L}_{\text{eff}} = -\frac{g_5^2}{M_{\mathcal{X}}^2} \epsilon_{\alpha\beta\gamma} [\bar{e}_j^c \bar{u}_{\alpha,i} Q_{\beta,i} Q_{\gamma,j} - \bar{d}_{\alpha,k}^c \bar{u}_{\beta,i} Q_{\gamma,i} L_k] + \text{h.c.} . \quad (23)$$

In the case of flipped SU(5) the $\mathcal{X}' = (X', Y')$ bosons form a (**3**^{*}, **2**, $-1/6$) representation of SU(3) \times SU(2) \times U(1) with couplings

$$\mathcal{L} = -i \frac{g_5}{\sqrt{2}} \mathcal{X}'_{\alpha\mu} [\epsilon_{\alpha\beta\gamma} \bar{Q}_\beta \gamma^\mu d_\gamma^c - \bar{u}_\alpha^c \gamma^\mu L] + \text{h.c.} . \quad (24)$$

Contrary to SU(5), there is only a single baryon and lepton number violating operator in flipped SU(5),

$$\mathcal{L}_{\text{eff}} = \frac{g_5^2}{M_{\mathcal{X}}'^2} \epsilon_{\alpha\beta\gamma} \bar{d}_{\alpha,k}^c \bar{u}_{\beta,i} Q_{\gamma,i} L_k + \text{h.c.} . \quad (25)$$

3.2 Effective operators in 6D models

In the orbifold model described above, the up-type quarks are localized at one fixed point each, in particular the up quark is located at the Georgi-Glashow one. It is therefore clear that dimension-6 proton decay can arise via the exchange of the SU(5) X and Y bosons as in the traditional 4D picture. There are though two important differences in the 6D case, as we will see in the following.

First we have to take into account the presence of not only one \mathcal{X} gauge boson, but of a Kaluza-Klein (KK) tower with masses given by

$$M_{\mathcal{X}}^2(n, m) = \frac{(2n+1)^2}{R_5^2} + \frac{(2m)^2}{R_6^2} , \quad (26)$$

for $n, m = 0, 1, 2, \dots$. The lowest possible mass is $M_{\mathcal{X}}(0, 0) = 1/R_5$, as given by the SU(5) breaking parity. Note that if we define the 4D gauge coupling as the effective coupling of

the zero modes, the KK modes interact more strongly by a factor $\sqrt{2}$ due to their bulk normalization.

To obtain the low energy effective operator, we then have to sum over the KK modes,

$$\begin{aligned} \frac{1}{(M_{\mathcal{X}}^{\text{eff}})^2} &= 2 \sum_{n,m=0}^{\infty} \frac{1}{M_{\mathcal{X}}^2(n,m)} \\ &= 2 \sum_{n,m=0}^{\infty} \frac{R_5^2}{(2n+1)^2 + \frac{R_5^2}{R_6^2}(2m)^2} . \end{aligned} \quad (27)$$

Taking formally the limit $R_6/R_5 \rightarrow 0$, we regain the 5D result [22],

$$\frac{1}{(M_{\mathcal{X}}^{\text{eff}})^2} = 2 \sum_{n=0}^{\infty} \frac{R_5^2}{(2n+1)^2} = \frac{\pi^2 R_5^2}{4} . \quad (28)$$

The double sum in Eq. (27) is logarithmically divergent. Since our model is valid only below the scale M_* , where it becomes strongly coupled and also 6D gravity corrections are no longer negligible, we restrict the sum to masses $M_{\mathcal{X}}(n,m) \leq M_*$. One easily finds

$$\frac{1}{(M_{\mathcal{X}}^{\text{eff}})^2} = \frac{\pi}{4} R_5 R_6 \left(\ln(M_* R_5) + C \left(\frac{R_5}{R_6} \right) + \mathcal{O} \left(\frac{1}{R_{5/6} M_*} \right) \right) . \quad (29)$$

Note that in the logarithm the smallest KK mass appears, $R_5 = 1/M_{\mathcal{X}}(0,0)$. The dependence of $1/(M_{\mathcal{X}}^{\text{eff}})^2$ on the cutoff M_* has to disappear once the model is embedded in a more fundamental theory. In the symmetric case, $R_5 = R_6 = 1/M_c$, one finds $C(1) \simeq 2.3$ and the expression (29) simplifies to

$$\frac{1}{(M_{\mathcal{X}}^{\text{eff}})^2} \simeq \frac{\pi}{4 M_c^2} \left(\ln \left(\frac{M_*}{M_c} \right) + 2.3 \right) . \quad (30)$$

Numerically, this agrees with the explicit sum over the KK masses within 1% for $M_*/M_c = 10 \dots 50$, which is the relevant range for the ratio of cutoff and compactification scales in 6D.

The second, most important difference of 6D models compared to 4D models is the non-universal coupling of the \mathcal{X} gauge bosons. In fact, due to the parities and the $\text{SO}(10)$ breaking pattern, their wavefunctions must vanish on the fixed points with broken $\text{SU}(5)$ symmetry, O_{ps} and O_{fl} , and therefore no coupling arises via the kinetic term with the charm and top quark or to the brane states $d_{2,3}^c, l_{2,3}$. We also have couplings to the bulk states d_4^c, d_4 and l_4, l_4^c . However, due to the embedding of the zero modes in full $\text{SU}(5)$ multiplets together with massive KK modes, i.e. (d_4^c, L_4) , (d_4, L_4^c) , (D_4^c, l_4) and (D_4, l_4^c) , the charged current interaction always mixes the light states with the heavy ones, and it is therefore irrelevant for the low energy process of proton decay [22]. So the kinetic coupling in Eq. (23) arises only for a single flavour eigenstate, not for all flavours as in the usual 4D case.

3.3 Corrections from derivative brane operators

Apart from the kinetic term couplings, at any brane additional couplings can arise containing derivatives along the extra dimensions of the locally vanishing gauge bosons. Such operators are a 6D generalization of the 5D derivative operators discussed in [22, 32],

$$\mathcal{L}_d = \sum_{\text{fixed points}} \delta_i(z) \frac{c_{5/6}^i}{M_*} \int_{\theta^2 \bar{\theta}^2} \bar{\Phi}_1 (\mathcal{D}_{5/6} e^{2V}) \Phi_2 + \text{h.c.} \quad (31)$$

Here $c_{5/6}^i$ are unknown brane coefficients, $\mathcal{D}_{5/6} = \partial_{5/6} + iA_{5/6}$ are the covariant derivatives in the extra dimensions and Φ_i are any two different, locally non-vanishing fields in group representations which form a singlet together with generators of the broken symmetries. For unbroken symmetries the chiral superfields $A_{5/6}$ vanish at the fixpoints.

These supersymmetric terms produce on the GG brane couplings with the flipped SU(5) leptoquark gauge bosons \mathcal{X}' , whose derivatives do not vanish on that brane. On the flipped SU(5) brane, there are couplings containing the derivative of the \mathcal{X} gauge bosons, and on the Pati-Salam brane there are derivative couplings with both \mathcal{X}' and \mathcal{X} . Due to these additional vertices, three different classes of operators can arise:

- operators coming from \mathcal{X}' exchange on the GG brane: these involve two derivative vertices and can produce additional contributions to the effective operator

$$\overline{d_k^c} \overline{u_1^c} Q_1 L_j \quad (32)$$

with $k, j = 1, 4$; we will discuss their contribution below;

- operators coming from \mathcal{X} -exchange on the flipped SU(5) brane or $\mathcal{X}, \mathcal{X}'$ exchange on the Pati-Salam brane: these usually involve the charm and top quark instead of the up quark, and they are therefore irrelevant for proton decay;
- interbrane operators from both the exchanges of \mathcal{X} and \mathcal{X}' gauge bosons: they can involve either one or two derivative vertices and generate mixed flavour operators of the type

$$\overline{e_j^c} \overline{u_1^c} u_1 d_k - \overline{d_k^c} \overline{u_1^c} Q_1 L_j \quad k, j = 2, 3, 4 \quad \mathcal{X} \text{ exchange}, \quad (33)$$

$$\overline{d_2^c} \overline{u_1^c} d_2 \nu_k \quad k = 1, 4 \quad \mathcal{X}' \text{ exchange GG—fl}, \quad (34)$$

$$\overline{d_j^c} \overline{u_1^c} d_l \nu_k \quad j, l = 3, 4; k = 1, 4 \quad \mathcal{X}' \text{ exchange GG—PS}. \quad (35)$$

Apart from the last term, they are usually suppressed compared to the kinetic term operators by a factor M_c/M_* due to the different parities of the vertices.

To estimate the effect of these additional operators, which introduce a dependence on the $\mathcal{O}(1)$ coefficients $c_{5/6}$, let us now consider the KK summations with one or two derivative vertices. We restrict ourselves here to the case $R_5 = R_6 = 1/M_c$ and universal coefficients $c_{5/6}$ at the different fixpoints. Note that even if suppressed by M_* , these operators can be as important as the usual ones, since the derivative enhances the divergence of the KK summation, which compensates the suppression. For example, from the exchange of the \mathcal{X}' bosons on the GG brane, we obtain the sum

$$\frac{1}{(M_{\mathcal{X}'}^{\text{eff}})_{\text{b.o.}}^2} = \frac{2}{M_*^2} \sum_{n,m} \frac{|c_5(2n+1) + c_6(2m+1)|^2}{(2n+1)^2 + (2m+1)^2}, \quad (36)$$

which is quadratically divergent. Using again the cutoff $M_{\mathcal{X}}(n, m) \leq M_*$, we obtain

$$\frac{1}{(M_{\mathcal{X}'}^{\text{eff}})_{\text{b.o.}}^2} = \frac{\pi}{16M_c^2} \left(|c_5|^2 + |c_6|^2 + \frac{4}{\pi} \text{Re}[c_5 c_6^*] + \mathcal{O}\left(\frac{M_c}{M_*}\right) \right), \quad (37)$$

to be compared with the ‘canonical’ term Eq. (30). A similar result is obtained for the exchange of \mathcal{X}' gauge bosons between the GG and the PS brane, affecting only the decay into neutrinos.

The exchange of gauge bosons between different branes involving only one single derivative operator are less dangerous since the propagator gives a factor $(-1)^n$ accounting for the different parities of the derivative and the kinetic term vertices. Therefore the KK summations are in general suppressed by a factor M_c/M_* . The exchange of \mathcal{X} bosons between the GG and the flipped SU(5) brane gives

$$\frac{1}{(M_{\mathcal{X}}^{\text{eff}})_{\text{b.o.}}^2} = \frac{2}{M_c M_*} \sum_{n,m} (-1)^n \frac{c_5(2n+1) + c_6(2m)}{(2n+1)^2 + (2m)^2}. \quad (38)$$

This sum is only logarithmically divergent thanks to the alternating signs. Using again the cutoff $M_{\mathcal{X}}(n, m) \leq M_*$, one finds

$$\frac{1}{(M_{\mathcal{X}}^{\text{eff}})_{\text{b.o.}}^2} = \frac{1}{2M_c M_*} \left(c_6 \ln\left(\frac{M_*}{M_c}\right) + \mathcal{O}(1) \right), \quad (39)$$

which is suppressed compared to the ‘canonical’ term by a factor M_c/M_* . The same result is obtained for the \mathcal{X}' exchange between the GG and the flipped SU(5) branes.

Note that in principle operators with a higher number of derivatives can also be present, which contribute at the same level as the single derivative ones because the divergence of the KK summation compensates the suppression by powers of M_* . We will assume that their contribution is small.

Regarding the N=2 scalar superpartners of the SU(5) gauge bosons, $\mathcal{X}_{5,6}$, the brane terms in Eq. (31) give rise to couplings with fermion kinetic terms which can only produce

corrections of order $(m_p/M_*)^2$. The derivatives of the $\mathcal{X}_{5,6}$ bosons do not couple to fermion pairs and are therefore irrelevant.

Finally, we emphasize that the position of the lightest quark generation is crucial for the discussion of proton decay. For instance, if the up quark were located on the Pati-Salam brane, the dimension-6 operator coming from the kinetic terms would be absent since both the \mathcal{X} bosons of SU(5) and the \mathcal{X}' bosons of flipped SU(5) vanish there. In principle, this gives us a means to avoid the ‘canonical’ dimension-6 operators completely, leaving the derivative couplings as dominant contributions.

4 Flavour structure and branching ratios

4.1 Flavour mixing in 6D versus 4D GUT models

Proton decay involves only the light quark states and the operators containing the combinations uud and udd . Therefore we have to rotate the weak eigenstates into the mass eigenstates and single out the contributions for the lightest generation. Without loss of generality and for future convenience, we can start in the basis where the up-quark mass matrix is diagonal. Then the down quark and lepton mass matrices are not diagonal, in general, but can be diagonalised by unitary transformations,

$$d_L = U_L^d d'_L, \quad e_L = U_L^e e'_L, \quad \nu_L = U_L^\nu \nu'_L, \quad (40)$$

$$d_R = U_R^d d'_R, \quad e_R = U_R^e e'_R, \quad (41)$$

where the prime denotes mass eigenstates. Since the up-quark matrix is diagonal, U_L^d coincides with the CKM matrix.

We can now express the proton decay operators of Eq. (23) in term of mass eigenstates,

$$\begin{aligned} \mathcal{L}_{\text{eff}} = \frac{g_5^2}{M_{\mathcal{X}}^2} \epsilon_{\alpha\beta\gamma} \Big[& \overline{e'_k} (U_R^{e\top})_{kj} \overline{u}_{\alpha,i}^c \left(d'_{\beta,m} (U_L^d)_{im} u_{\gamma,j} - u_{\beta,i} (U_L^d)_{jl} d'_{\gamma,l} \right) \\ & + \overline{d'_{\alpha,l}} (U_R^{d\top})_{lk} \overline{u}_{\beta,i}^c \left(u_{\gamma,i} (U_L^e)_{kj} e'_j - d'_{\gamma,m} (U_L^d)_{im} (U_L^\nu)_{kj} \nu'_j \right) \Big] + \text{h.c.} \quad (42) \end{aligned}$$

Note that for the orbifold construction, where only the first generation weak eigenstates couple to the \mathcal{X} bosons, the effective operators read instead

$$\begin{aligned} \mathcal{L}_{\text{eff}} = \frac{g_5^2}{(M_{\mathcal{X}}^{\text{eff}})^2} \epsilon_{\alpha\beta\gamma} \Big[& 2 \overline{e'_k} (U_R^{e\top})_{k1} \overline{u}_{\alpha,1}^c d'_{\beta,m} (U_L^d)_{1m} u_{\gamma,1} \\ & + \overline{d'_{\alpha,l}} (U_R^{d\top})_{l1} \overline{u}_{\beta,1}^c \left(u_{\gamma,1} (U_L^e)_{1j} e'_j - d'_{\gamma,m} (U_L^d)_{1m} (U_L^\nu)_{1j} \nu'_j \right) \Big] + \text{h.c.} \quad (43) \end{aligned}$$

Let us analyze the mixing pattern for the down quarks in the orbifold model. Since the mass matrices of down quarks and charged leptons both have the form Eq. (4), $m^d \sim m^e \sim m$, U_R^d and U_L^e have the same structure but, in general, coefficients $\mathcal{O}(1)$ will be different. For $\mu_1, \mu_2 \ll \mu_3$, we obtain for the right-handed down-type quarks and left-handed charged leptons,

$$U_R^d \sim U_L^e \sim V_4 V_3 = \begin{pmatrix} -\frac{\tilde{M}_2}{M_{12}} & \frac{\tilde{M}_1(\tilde{\mu}_3\tilde{M}_3 - \mu_3\tilde{M}_4)}{\tilde{\mu}_3\tilde{M}M_{12}} & -\frac{\tilde{M}_1(\tilde{\mu}_3\tilde{M}_4 + \mu_3\tilde{M}_3)}{\tilde{\mu}_3\tilde{M}^2} & \frac{\tilde{M}_1}{\tilde{M}} \\ \frac{\tilde{M}_1}{M_{12}} & \frac{\tilde{M}_2(\tilde{\mu}_3\tilde{M}_3 - \mu_3\tilde{M}_4)}{\tilde{\mu}_3\tilde{M}M_{12}} & -\frac{\tilde{M}_2(\tilde{\mu}_3\tilde{M}_4 + \mu_3\tilde{M}_3)}{\tilde{\mu}_3\tilde{M}^2} & \frac{\tilde{M}_2}{\tilde{M}} \\ 0 & -\frac{\tilde{\mu}_3}{\mu_3} \frac{\tilde{M}_{12}}{\tilde{M}} & -\frac{\tilde{\mu}_3\tilde{M}_3\tilde{M}_4 - \mu_3(\tilde{M}_1^2 + \tilde{M}_2^2 + \tilde{M}_4^2)}{\tilde{\mu}_3\tilde{M}^2} & \frac{\tilde{M}_3}{\tilde{M}} \\ 0 & \frac{\mu_3}{\tilde{\mu}_3} \frac{\tilde{M}_{12}}{\tilde{M}} & \frac{\tilde{\mu}_3(\tilde{M}_1^2 + \tilde{M}_2^2 + \tilde{M}_3^2) - \mu_3\tilde{M}_3\tilde{M}_4}{\tilde{\mu}_3\tilde{M}^2} & \frac{\tilde{M}_4}{\tilde{M}} \end{pmatrix}, \quad (44)$$

up to the two-dimensional mixing matrix for the second and third generation discussed in Section 2.

The rotation matrices of the left-handed down quarks and right-handed leptons are obtained by diagonalizing $m^\top m$, which leads to small mixing angles, with

$$U_L^d = V_{\text{CKM}} \sim U_R^e. \quad (45)$$

The unitary matrices U_L^e , U_R^d , U_L^d and U_R^e determine the coefficients of the proton decay operators in Eq. (43).

To make a comparison with ordinary 4D GUT models, we consider the flavour structure of two $\text{SU}(5)$ models described in Refs. [33, 34]. These models make use of the Froggatt-Nielsen mechanism [35] where a global $\text{U}(1)_F$ flavour symmetry is broken spontaneously by the VEV of gauge singlet field Φ at a high scale. Then the Yukawa couplings arise from the non-renormalizable operators,

$$h_{ij} = g_{ij} \left(\frac{\langle \Phi \rangle}{\Lambda} \right)^{Q_i + Q_j}. \quad (46)$$

Here, g_{ij} are couplings $\mathcal{O}(1)$ and Q_i are the $\text{U}(1)_F$ charges of the various fermions. Particularly interesting is the case with a ‘lopsided’ family structure, where the chiral charges are different for $\mathbf{5}^*$ and $\mathbf{10}$ of the same family. The two examples [33, 34] with phenomenologically allowed lopsided charges are given in Table 1.

Note that in these models the large neutrino mixing is explained by a large mixing of $\mathbf{5}^*$ -plets, which is analogous to the large mixing of lepton doublets and right-handed down quarks in the 6D model described above. Contrary to the 6D model, this does not determine the $\text{U}(1)_F$ charges of the right-handed neutrinos. For proper choices these models also lead to successful baryogenesis via leptogenesis [36].

Q_F	$\mathbf{10}_3$	$\mathbf{10}_2$	$\mathbf{10}_1$	$\mathbf{5}_3^*$	$\mathbf{5}_2^*$	$\mathbf{5}_1^*$
model A	0	1	2	a	a	$a + 1$
model B	0	3	5	0	0	2

Table 1: $U(1)_F$ charges of the $SU(5)$ fields; $a = 0, 1$.

The charge assignments determine the structure of the Yukawa matrices. In model A [33], corresponding to the semi-anarchical model of [34], the couplings for down quarks and charged leptons read

$$h_d \sim h_e \sim \epsilon^a \begin{pmatrix} \epsilon^3 & \epsilon^2 & \epsilon^2 \\ \epsilon^2 & \epsilon & \epsilon \\ \epsilon & 1 & 1 \end{pmatrix}, \quad (47)$$

where the parameter $\epsilon = \langle \Phi \rangle / \Lambda \sim 1/17$ controls the flavour mixing. Diagonalisation of the Yukawa matrices yields

$$U_L^d = V_{\text{CKM}} \sim U_R^e \sim \begin{pmatrix} 1 & \epsilon & \epsilon^2 \\ \epsilon & 1 & \epsilon \\ \epsilon^2 & \epsilon & 1 \end{pmatrix}, \quad U_R^d \sim U_L^e \sim \begin{pmatrix} 1 & \epsilon & \epsilon \\ \epsilon & 1 & 1 \\ \epsilon & 1 & 1 \end{pmatrix}. \quad (48)$$

In model B, which corresponds to the hierarchical H_{II} model of [34], the structure is similar, while the small parameter is instead $\lambda \sim 0.35$, such that $\lambda^2 \sim \epsilon$.

4.2 Decay rates and branching ratios

To calculate the decay rates, we have to evaluate the hadron matrix elements $\langle PS | \mathcal{O} | p \rangle$, which describe the transition from the proton via the three-quark operator \mathcal{O} to a pseudo scalar meson. The various matrix elements are calculated from the basic element

$$\alpha P_L u_p = \epsilon_{\alpha\beta\gamma} \left\langle 0 \left| \left(d_R^\alpha u_R^\beta \right) u_L^\gamma \right| p \right\rangle \quad (49)$$

with the aid of chiral perturbation theory [37, 38]; u_p denotes the proton spinor. The decay rates for the different channels are given in Table 2. Here m_p , m_π , m_K and m_η denote the masses of proton, pion, kaon and eta, respectively, and f_π is the pion decay constant; $m_B = 1.15 \text{ GeV}$ is an average baryon mass according to contributions from diagrams with virtual Σ and Λ ; $D = 0.80$ and $F = 0.46$ are the symmetric and antisymmetric $SU(3)$ reduced matrix elements for the axial-vector current [39]. The matrix element α is evaluated by means of lattice QCD simulations; its absolute value varies in the range $(0.003 - 0.03) \text{ GeV}^3$. We will choose $|\alpha| = 0.01 \text{ GeV}^3$ (see the recent discussion in Ref. [40]).

$$\begin{aligned}
\Gamma(p \rightarrow e_j^+ \pi^0) &= \frac{(m_p^2 - m_{\pi^0}^2)^2}{32\pi m_p^3 f_\pi^2} \alpha^2 A^2 G_G^2 \left(\frac{1 + D + F}{\sqrt{2}} \right)^2 C_{udue_j}^2 \\
\Gamma(p \rightarrow \bar{\nu}_j \pi^+) &= \frac{(m_p^2 - m_{\pi^\pm}^2)^2}{32\pi m_p^3 f_\pi^2} \alpha^2 A^2 G_G^2 (1 + D + F)^2 C_{udd\nu_j}^2 \\
\Gamma(p \rightarrow e_j^+ K^0) &= \frac{(m_p^2 - m_{K^0}^2)^2}{32\pi m_p^3 f_\pi^2} \alpha^2 A^2 G_G^2 \left(1 + (D - F) \frac{m_p}{m_B} \right)^2 C_{usue_j}^2 \\
\Gamma(p \rightarrow \bar{\nu}_j K^+) &= \frac{(m_p^2 - m_{K^\pm}^2)^2}{32\pi m_p^3 f_\pi^2} \alpha^2 A^2 G_G^2 \left[\left(\frac{2}{3} D \frac{m_p}{m_B} \right) C_{usd\nu_j} + \left(1 + \frac{D + 3F}{3} \frac{m_p}{m_B} \right) C_{uds\nu_j} \right]^2 \\
\Gamma(p \rightarrow e_j^+ \eta) &= \frac{(m_p^2 - m_\eta^2)^2}{32\pi m_p^3 f_\pi^2} \alpha^2 A^2 G_G^2 \left(\frac{1 + D - 3F}{\sqrt{6}} \right)^2 C_{udue_j}^2
\end{aligned}$$

Table 2: Partial widths of proton decay channels [41].

In the decay rates listed in Table 2 the coupling constant $G_G = g_5^2/(M_\chi^{\text{eff}})^2$ is given by Eqs. (30), (37) and (39). The operators have to be evolved from the GUT scale down to the hadronic scale, which is described by the factor $A = A^{\text{SD}} \cdot A^{\text{LD}}$. It contains both a short-distance contribution $A^{\text{SD}} = 2.37$, for the evolution from the GUT scale to the SUSY-breaking scale, and a long-distance contribution $A^{\text{LD}} = 1.43$, for the evolution from the SUSY-breaking scale to 1 GeV [13]. The effect of lepton masses is neglected.

The quark and lepton mixing patterns discussed above fix the coefficients C_{ijk}^2 in the decay rates. As an example, for the process $p \rightarrow e^+ \pi^0$, we obtain from Eq. (43),

$$C_{udue}^2 = 4 [(U_R^e)_{11} (U_L^d)_{11}]^2 + [(U_R^d)_{11} (U_L^e)_{11}]^2. \quad (50)$$

The coefficients for the other processes can be read off analogously. The decay rates in Table 2 have the same form as the decay rates determined by dimension-5 operators. The difference lies in the coefficients C_{ijk} and the coupling constant G_G .

We now start with the simplest case of our orbifold model, with $U_R^d = U_L^e$, and with degenerate masses \widetilde{M} and $\widetilde{\mu}_3 = \mu_3$, which we denote as case I. The mixing matrix for right-handed down quarks and left-handed charged leptons, Eq. (44), is then simply given by

$$U_R^d = U_L^e = \begin{pmatrix} -\frac{1}{\sqrt{2}} & 0 & -\frac{1}{2} & \frac{1}{2} \\ \frac{1}{\sqrt{2}} & 0 & -\frac{1}{2} & \frac{1}{2} \\ 0 & -\frac{1}{\sqrt{2}} & \frac{1}{2} & \frac{1}{2} \\ 0 & \frac{1}{\sqrt{2}} & \frac{1}{2} & \frac{1}{2} \end{pmatrix}, \quad (51)$$

decay channel	Branching Ratios [%]		
	6D SO(10) case I	case II	SU(5) \times U(1) _F models A & B
$e^+\pi^0$	75	71	54
$\mu^+\pi^0$	4	5	< 1
$\bar{\nu}\pi^+$	19	23	27
e^+K^0	1	1	< 1
μ^+K^0	< 1	< 1	18
$\bar{\nu}K^+$	< 1	< 1	< 1
$e^+\eta$	< 1	< 1	< 1
$\mu^+\eta$	< 1	< 1	< 1

Table 3: Resulting branching ratios and comparison with SU(5) \times U(1)_F.

thus the state d_1^c has no strange-component. For the current-current operators we then obtain from Eq. (43),

$$\begin{aligned}
\mathcal{L}_{\text{eff}} \simeq \frac{g_5^2}{(M_{\tilde{\chi}}^{\text{eff}})^2} \epsilon_{\alpha\beta\gamma} \Bigg[& 2 V_{ud}^2 \bar{e}^c \bar{u}_\alpha^c d_\beta u_\gamma + \frac{1}{2} \bar{d}_\alpha^c \bar{u}_\beta^c u_\gamma e + 2 V_{ud} V_{us} \bar{\mu}^c \bar{u}_\alpha^c d_\beta u_\gamma \\
& + 2 V_{ud} V_{us} \bar{e}^c \bar{u}_\alpha^c s_\beta u_\gamma + 2 V_{us}^2 \bar{\mu}^c \bar{u}_\alpha^c s_\beta u_\gamma \\
& - \sum_{j=1}^3 \frac{1}{\sqrt{2}} (U_L^\nu)_{1j} \bar{u}_\alpha^c \bar{d}_\beta^c \left\{ V_{ud} d_\gamma + V_{us} s_\gamma \right\} \nu_j \Bigg] + \text{h.c.} , \quad (52)
\end{aligned}$$

where the fermions are now mass eigenstates. From this equation we can read off the coefficients of the various coefficients C_{ijklm} appearing in the decay rates (cf. Table 2),

$$\begin{aligned}
C_{udue}^2 &= 4 V_{ud}^4 + \frac{1}{4} , & C_{us\mu\mu}^2 &= 4 V_{us}^4 , & C_{udu\mu}^2 &= C_{usue}^2 = 4 V_{us}^2 V_{ud}^2 , \\
C_{udd\nu}^2 &= \frac{1}{2} V_{ud}^2 , & C_{udsv} &= \frac{1}{\sqrt{2}} V_{us} , & C_{usd\nu} &= 0 , \quad (53)
\end{aligned}$$

where we have used $\sum_{j=1}^3 (U_L^\nu)_{1j} (U_L^\nu)_{1j}^* = 1$.

The numerical results for the branching ratios are listed in Table 3. Note that the effect of the derivative operators is negligible for $c_5 = c_6 = 1$. For the listed branching ratios the corrections are less than 3%.

To compare the branching ratios of the 6D model with those of the two 4D GUT models described above, we assume that some mechanism suppresses or avoids the proton decay arising from dimension-5 operators. The coefficients C_{ijkl}^2 can then be derived from Eq. (42) using the mixing matrices given in Eq. (48). For model A, they read

$$\begin{aligned}
C_{udue}^2 &\simeq C_{usu\mu}^2 \simeq 4, & C_{ud\mu\mu}^2 &\simeq C_{usue}^2 \simeq 4\epsilon^2, \\
C_{udd\nu}^2 &\simeq \frac{1}{2}, & C_{uds\nu} &\simeq \frac{1}{\sqrt{2}}, & C_{usd\nu} &\simeq 2\epsilon. \quad (54)
\end{aligned}$$

In model B, ϵ is replaced by λ^2 . The differences between the branching ratios of the two models are not significant.

The difference between the 6D SO(10) and the 4D SU(5) models is most noticeable in the channel $p \rightarrow \mu^+ K^0$. This is due to the absence of second and third generation weak eigenstates in the current-current operators and the vanishing (12)-component in U_R^d and U_L^e in the case of the 6D model. Hence, the decay $p \rightarrow \mu^+ K^0$ is doubly Cabibbo suppressed. This effect is a direct consequence of the localization of the ‘first generation’ to the Georgi-Glashow brane.

Let us now consider the general case, where the $\widetilde{M}^{(d,e)}$ are not degenerate, and where μ_3 and $\widetilde{\mu}_3^{(d,e)}$ differ as well. From Eq. (44) we see that the strange component in d_1^c does not vanish anymore, but it is smaller than the bottom component. We have studied several cases whose results agree remarkably well. As an illustration, consider the case where $\widetilde{\mu}_3^d = 2\mu_3$ and $\widetilde{\mu}_3^e = 3\mu_3$, with non-degenerate heavy masses $\widetilde{M}_1^d : \widetilde{M}_2^d : \widetilde{M}_3^d : \widetilde{M}_4^d = \frac{1}{2} : \frac{1}{\sqrt{2}} : \frac{1}{\sqrt{2}} : 1$ and $\widetilde{M}_1^e : \widetilde{M}_2^e : \widetilde{M}_3^e : \widetilde{M}_4^e = \frac{1}{2} : \frac{1}{\sqrt{2}} : 1 : \frac{1}{2}$ (case II). The branching ratios are listed in Table 3; the differences between the two cases are indeed small.

The most striking difference is the decay channel $p \rightarrow \mu^+ K^0$, which is suppressed by about two orders of magnitude in the 6D model with respect to 4D models. It is therefore important to determine an upper limit for this channel in the 6D model. Varying the mass parameters in the range $\widetilde{M}_j/\widetilde{M} = 0.1 - 1$ and $\widetilde{\mu}_3^{d,e}/\mu_3 = 0.1 - 10$, we find

$$\frac{\Gamma(p \rightarrow \mu^+ K^0)}{\Gamma(p \rightarrow e^+ \pi^0)} \lesssim 5\% . \quad (55)$$

Finally, a limit on the compactification scale can be derived from the decay width of the dominant channel $p \rightarrow e^+ \pi^0$. Neglecting the suppressed contributions from the derivative operators, we obtain the analytic expression

$$\begin{aligned}
\Gamma(p \rightarrow e^+ \pi^0) &\simeq \frac{(m_p^2 - m_{\pi^0}^2)^2}{32\pi m_p^3 f_\pi^2} \alpha^2 A^2 \left(\frac{1 + D + F}{\sqrt{2}} \right)^2 \\
&\times \frac{\pi^2}{16 M_c^4} \left(\ln \left(\frac{M_*}{M_c} \right) + 2.3 \right)^2 \left[4V_{ud}^4 + \frac{\widetilde{M}_2^{d2}}{\widetilde{M}_1^{d2} + \widetilde{M}_2^{d2}} \frac{\widetilde{M}_2^{e2}}{\widetilde{M}_1^{e2} + \widetilde{M}_2^{e2}} \right] \\
&\simeq \left(\frac{9 \times 10^{15} \text{ GeV}}{M_c} \right)^4 \left(\frac{\alpha}{0.01 \text{ GeV}^3} \right)^2 (5.3 \times 10^{33} \text{ yrs})^{-1} . \quad (57)
\end{aligned}$$

With $M_* = 10^{17} \text{ GeV}$ and $\widetilde{M}_{1,2}^{d,e} = \mathcal{O}(1)$, the experimental limit $\tau \geq 5.3 \times 10^{33}$ yields $M_c \geq M_c^{\min} \simeq 9 \times 10^{15} \text{ GeV}$, which is very close to the 4D GUT scale. The lower bound corresponds to $M_*/M_c^{\min} = 12$ and $(M_\chi^{\text{eff}})^2/(M_c^{\min})^2 = 3.72$.

5 Conclusions

We have studied proton decay in a 6D $\text{SO}(10)$ orbifold GUT model, which is determined by dimension-6 operators. The characteristic features of the model are the different breakings of the $\text{SO}(10)$ symmetry at different points in the extra dimensions and the associated localization of some quarks and leptons. We find that, like in 5D orbifold GUTs [22], the proton decay rate is enhanced and the branching ratios are strongly affected by the quark-lepton ‘geography’.

The summation over Kaluza-Klein towers depends logarithmically on the cutoff scale M_* in 6D, contrary to 5D, where the sum is finite. Identifying the cutoff with the 6D Planck mass, i.e. $M_* \simeq 10^{17}$ GeV, the SuperKamiokande bound on the proton lifetime leads to the lower bound on the compactification scale $M_c > 9 \times 10^{15}$ GeV. On the other hand, the approximate unification of gauge couplings suggests $M_c \simeq_{\text{GUT}} \simeq 2 \times 10^{16}$ GeV. This yields the proton lifetime $\tau(p \rightarrow e^+ \pi^0) \simeq 1 \times 10^{35}$ yrs which, remarkably, lies within the reach of the next generation of large volume detectors!

The peculiar flavour structure of our orbifold GUT model leads to characteristic signatures in the branching ratios of proton decay, in particular the strong suppression of the mode $p \rightarrow \mu^+ K^0$ compared to the predictions of 4D models. The reason is the higher-dimensional quark-lepton ‘geography’ and the related non-universal couplings of GUT bosons to fermions. Such a pattern can be tested already with a handful of events! Hence, the discovery of proton decay may not only confirm the most striking prediction of grand unification, but it might also reveal its higher dimensional origin.

We would like to thank A. Hebecker for helpful discussions. L.C. would also like to thank J. Ellis, and A. Romanino, C. Scrucca and the other participants of the CERN Phen Club on 26/2/2004 for useful discussions and suggestions. The work of D.E.C. was supported by Fundação para a Ciência e a Tecnologia under the grant SFRH/BPD/1598/2000.

References

- [1] J. C. Pati and A. Salam, Phys. Rev. **D 10** (1974) 275.
- [2] H. Georgi and S. L. Glashow, Phys. Rev. Lett. **32** (1974) 438.
- [3] H. Georgi, Particles and Fields 1974, ed. C. E. Carlson (AIP, NY, 1975) p. 575.
- [4] H. Fritzsch, P. Minkowski, Ann. Phys. 93 (1975) 193.
- [5] S. M. Barr, Phys. Lett. **B 112** (1982) 219.
- [6] J. P. Derendinger, J. E. Kim, D. V. Nanopoulos, Phys. Lett. **B 139** (1984) 170
- [7] Y. Suzuki *et al.* [TITAND Working Group Collaboration], arXiv:hep-ex/0110005.
- [8] K. S. Ganezer [Super-Kamiokande Collaboration], Int. J. Mod. Phys. A **16S1B** (2001) 855.
- [9] T. Goto and T. Nihei, Phys. Rev. **D 59** (1999) 115009.
- [10] R. Dermisek, A. Mafi, S. Raby, Phys. Rev. **D 63** (2000) 03500.
- [11] H. Murayama and A. Pierce, Phys. Rev. **D 65** (2002) 055009.
- [12] B. Bajc, P. Fileviez Perez, G. Senjanović, Phys. Rev. **D 66** (2002) 075005.
- [13] D. Emmanuel-Costa and S. Wiesenfeldt, Nucl. Phys. **B 661** (2003) 62.
- [14] C. Jarlskog, Phys. Lett. **B 82** (1979) 401.
- [15] R. N. Mohapatra, Phys. Rev. Lett. **43** (1979) 893.
- [16] J. Ellis, M. K. Gaillard and D. V. Nanopoulos, Phys. Lett. **B 88** (1979) 320.
- [17] Y. Achiman and M. Richter, Phys. Lett. **B 523** (2001) 304.
- [18] J. Ellis, D. V. Nanopoulos and J. Walker, Phys. Lett. **B 550** (2002) 99.
- [19] P. Fileviez Pérez, hep-ph/0403286.
- [20] G. Altarelli and F. Feruglio, Phys. Lett. B **511** (2001) 257.
- [21] L. J. Hall and Y. Nomura, Phys. Rev. **D 64** (2001) 055003.
- [22] A. Hebecker and J. March-Russell, Phys. Lett. **B 539** (2002) 119.
- [23] T. Asaka, W. Buchmüller and L. Covi, Phys. Lett. **B 563** (2003) 209.

- [24] T. Kobayashi, S. Raby and R.-J. Zhang, hep-ph/0403065.
- [25] S. Förste, H.-P. Nilles, P. Vaudrevange, A. Wingerter, hep-th/0406208.
- [26] T. Asaka, W. Buchmüller and L. Covi, Phys. Lett. **B 523** (2001) 199.
- [27] L. J. Hall, Y. Nomura, T. Okui and D. R. Smith, Phys. Rev. **D 65** (2002) 035008.
- [28] T. Asaka, W. Buchmüller and L. Covi, Nucl. Phys. **B 648** (2003) 231.
- [29] For a recent review, see
C. A. Scrucca, M. Serone, hep-th/0403163.
- [30] R. Fleischer, Phys. Rep. **370C** (2002) 537.
- [31] H. Fritzsch, Z. Xing, Prog. Part. Nucl. Phys. **45** (2000) 1.
- [32] A. Hebecker, Nucl. Phys. **B 632** (2002) 101.
- [33] T. Yanagida, J. Sato, Nucl. Phys. Proc. Suppl. **77** (1999) 293.
- [34] G. Altarelli, F. Feruglio and I. Masina, hep-ph/0405048.
- [35] C. D. Froggatt and H. B. Nielsen, Nucl. Phys. **B 147** (1979) 277.
- [36] W. Buchmüller, T. Yanagida, Phys. Lett. **B 445** (1999) 399.
- [37] M. Claudson, M. B. Wise and L. J. Hall, Nucl. Phys. B **195** (1982) 297.
- [38] S. Chadha and M. Daniel, Nucl. Phys. B **229** (1983) 105.
- [39] N. Cabibbo, E. C. Swallow and R. Winston, hep-ph/0307298.
- [40] N. Tsutsui *et al.* [CP-PACS and JLQCD Collaborations], hep-lat/0402026.
- [41] S. Aoki *et al.* [JLQCD Collaboration], Phys. Rev. D **62** (2000) 014506.